Scanning Probe Microscopes

JG Kushmerick and PS Weiss, Pennsylvania State University, University Park, PA, USA

This article is reproduced from the previous edition, volume 3, pp 2043–2051, © 1999, Elsevier Ltd., with revisions made by the Editor.

Symbols

Å	Ångstrom
e	charge of an electron
E	energy
G_t	tunnelling conductance
I	tunnelling current
K	Kelvin
V	bias voltage
z	tip–sample separation
$\hbar$	Planck's constant/2π
Φ_{ap}	apparent barrier height
ω	vibrational frequency

The atomic resolution and spectroscopic capabilities of scanning probe microscopes (SPMs) have enabled elucidation of the great heterogeneity of surface sites including defects, step edges, lattice impurities, adsorbates, and grown structures. One or more of these minority sites often function as the active sites for surface processes, and their individual investigation is thus required to gain insight into such processes. Such specific information cannot typically be acquired by spectroscopies that measure ensemble averages of the surface.

The scanning tunnelling microscope (STM) is the most suited, and the most developed of the various SPMs, to perform local spectroscopic measurements. The development of STM in 1981 resulted in its inventors, Binnig and Rohrer, being awarded the Nobel prize for physics in 1986 (see Further Reading section). Discussion of STM techniques will constitute the bulk of this article. It also has the most restricted range of accessible substrates in terms of conductivity and roughness. The atomic force microscope (AFM) has limited spectroscopic capabilities but can image a wider range of samples. The near-field scanning optical microscope (NSOM) has excellent spectroscopic, but limited spatial resolution. These latter two SPMs are discussed at the end of this article.

The basic working principles of the STM rely on the quantum mechanical properties of electrons. When an atomically sharp metal probe tip is brought within a few Å of a conducting or semiconducting surface, electrons can tunnel through the energy barrier between the probe tip and surface. By applying a constant DC bias voltage (V), a net tunnelling current (I) can be induced between the probe tip and the sample under study. Raster scanning the tip across the surface, through the use of piezoelectric transducers while maintaining a constant tunnelling current, images a surface of constant density of electronic states. The resulting image is a convolution of topographic and electronic properties of the sample surface.

The tunnelling current is exponentially dependent on the tip–sample separation and linearly dependent on the densities of tip and sample electronic states. The applied bias voltage determines which electronic states, on the both sides of the tunnelling junction, are being sampled, and thus allows acquisition of *spatially resolved spectra*. Figure 1 is a schematic of the tunnelling potential barrier. Adjusting the bias voltage probes different electronic states, allowing the local density of states to be mapped as a function of energy. This is the basis of electronic spectroscopy with the STM.

Scanning Tunnelling Microscope

Experimental Methods

Voltage-Dependent Imaging

One straightforward means to gain spectroscopic information from the STM is to acquire multiple images of

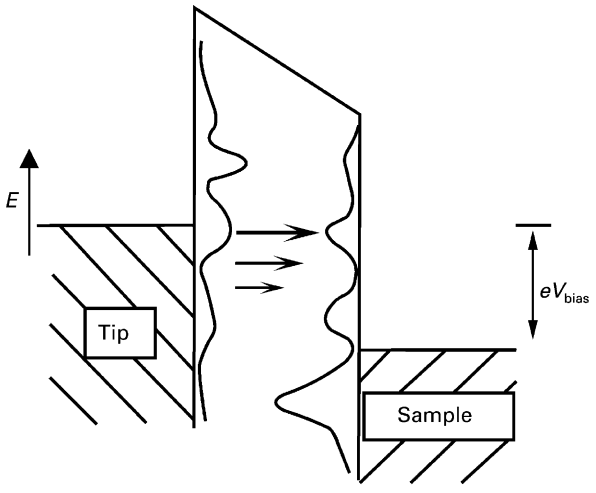

Figure 1 Energy level diagram for the tip–sample tunnelling gap, depicting electrons tunnelling from tip to sample. The local density of states for both the tip and sample as a function of energy is represented graphically.

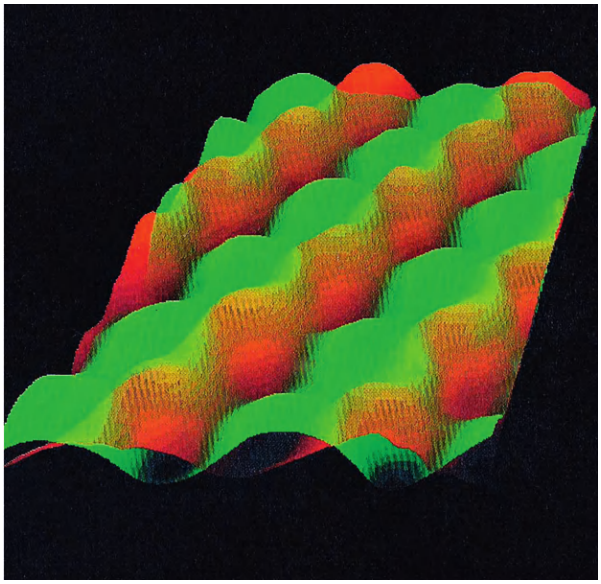

Figure 2 A composite of two images of the GaAs(110) surface. The orange features obtained at positive sample bias are the Ga atoms, while green features obtained at a negative sample bias are the As atoms. Feenstra RM, unpublished results.

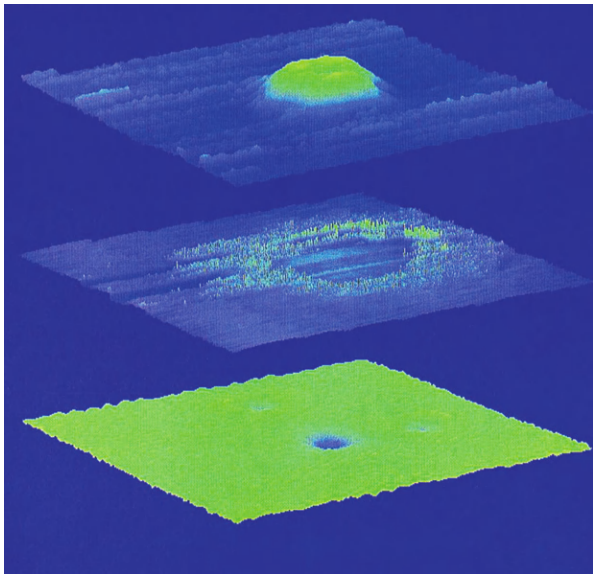

Figure 3 Three STM images of a Ni_3 cluster adsorbed on a MoS_2 basal plane at 4 K. All three images show a 60 Å × 60 Å area and are plotted as three-dimensional representations with the same aspect ratio and with the same angle of view. The images were acquired with sample biases of: +2 V (upper), +1.4 V (middle), and −2 V (lower). Reproduced with the permission of the American Chemical Society from Kushmerick JG and Weiss PS (1998) *Journal of Physical Chemistry B* 102: 10094–10097.

the same area sequentially at different bias voltage, and thus different energies. These images are then overlaid. Each image shows the relative contributions from features at the particular energy relative to the Fermi level defined by the bias voltage (at energies eV, where V is the bias voltage and e is the charge on an electron). Another method is to acquire tunnelling current vs. bias voltage (I–V) characteristics at every imaged point, or at selected locations.

A dramatic example of this technique is the contrast reversal observed for some semiconductor surfaces. When voltage-dependent imaging of GaAs(110) is performed, only the Ga atoms are imaged when electrons are tunnelling into surface states, while the As atoms are imaged when electrons are tunnelling from filled surface states to the tip. Figure 2 is a superposition of two images of the GaAs(110) surface. The orange image was obtained at positive sample bias, thus imaging the Ga atoms, while the green image was obtained with a negative sample bias, showing the As atoms. The cause of this contrast reversal is charge transfer from the Ga to the more electronegative As atoms, which results in the localization of the lowest lying empty states and highest lying filled states on the Ga and As atoms, respectively.

Voltage-dependent imaging can also be applied to understand bonding of adsorbate molecules to surfaces. Figure 3 shows a Ni_3 cluster on MoS_2 at a temperature of 4 K, imaged at three different bias voltages. The cluster's contribution to the electronic structure varies dramatically as can be seen at these different energies. At +2 V sample bias (electrons tunnelling into the empty states on the surface) the Ni_3 cluster appears as a significant protrusion from the MoS_2 surface, indicating that it enhances the local density of empty electronic states at this energy. Similarly, we see that the cluster depletes the local density of filled states at −2 V sample bias (electrons tunnelling from the filled sample electron states to the tip) since the cluster then appears as a depression in the surface. At a sample bias of +1.4 V the cluster is not directly apparent but a diffuse ring ∼30 Å in diameter surrounding it is imaged. This ring is outside the atomic positions of the Ni_3 cluster imaged at +2 V (∼16 Å diameter), and results from a perturbation of the MoS_2 surface electronic structure by the Ni_3 cluster. This ring is believed to be purely electronic in origin with little change in atomic positions of the substrate. Each image shows a different contribution of the Ni_3 cluster to the surface electronic structure, demonstrating how voltage-dependent imaging can measure electronic states as a function of both energy and position.

Voltage-dependent imaging can be a powerful technique but it does have some inherent problems. It is necessary to obtain many images in order to map the surface electronic structure as a function of energy. Thermal drift and piezoelectric creep can make overlay and comparison of successive images difficult. The fact that the constant current images acquired are a

convolution of geometric and electronic effects further complicates the interpretation of observed features. The latter technique of recording complete or selected sets of I–V characteristics, discussed in the next section, overcomes some of these problems.

Local Current–Voltage Measurements

Spectroscopic information over a large energy scale can be obtained by acquiring complete I–V curves at one or many locations. This can be accomplished by releasing feedback control while holding the probe tip steady and measuring the current with respect to applied bias voltage. Spectroscopy with the probe tip held in place allows scanning at both polarities and through zero bias.

Spectra are usually plotted as $(\mathrm{d}I/\mathrm{d}V)/(I/V)$ vs. V for comparison to other measurements of surface densities of states. This normalizes the spectra, removing the dependence on voltage and the exponential dependence on tip–sample separation. The derivative $\mathrm{d}I/\mathrm{d}V$ can be numerically calculated, or a lock-in amplifier can be used to measure $\mathrm{d}I/\mathrm{d}V$ phase sensitively, with a superimposed sinusoidal modulation on the bias voltage.

Synchronizing the feedback blanking and the applied voltage ramp enables acquisition of I–V curves at specified points in an image, thus mapping the energy and position dependence of the surface electronic structure in one image. **Figure 4** shows spectra acquired over Si atoms at three different locations in the unit cell of the Si(111)-(7 × 7) surface reconstruction. The three spectra show different electronic features due to the local bonding and environment of the Si atom probed.

Collection of data for the entire energy region of interest circumvents the need to construct a spectrum from several images. The dynamic signal range plays a role in determining how large an energy range can be scanned. The current goes to zero as the magnitude of the bias voltage decreases. Thus, features at high and low bias voltages can be hard to resolve in a single spectrum (recall that the preferred display of spectra, $(\mathrm{d}I/\mathrm{d}V)/(I/V)$ vs. V, has tunnelling current in the denominator).

Scanning Tunnelling Spectroscopy

Closely related to voltage-dependent tunnelling is the modulation technique of scanning tunnelling spectroscopy (STS). This technique consists of superimposing a small sinusoidal modulation voltage on the constant DC bias voltage. The modulation frequency is typically chosen to be higher than the cut-off frequency of the feedback loop, resulting in a constant average tunnelling current. If the modulation frequency is too low, the control electronics will attempt to compensate by adjusting the gap spacing. Alternatively, control of the tip height can be released during acquisition of spectra. By measuring the in-phase tunnelling current modulation with a lock-in amplifier, $\mathrm{d}I/\mathrm{d}V$ can be recorded simultaneously with the constant current image. Structure in $\mathrm{d}I/\mathrm{d}V$ as a function of the applied bias voltage can be attributed to structure in the local density of surface states.

Application of STS at constant average tunnelling current suffers from two disadvantages. The first is that the magnitude of the $\mathrm{d}I/\mathrm{d}V$ signal scales as I/V, and thus becomes progressively small at low bias voltages. The second is that at low bias voltages the tip–sample separation reduces in order to maintain a constant average tunnelling current. If the density of states is too low, the tip will come into contact and damage the surface. This form of STS, like voltage-dependent imaging, requires the acquisition of multiple images to map out electronic structure as a function of energy.

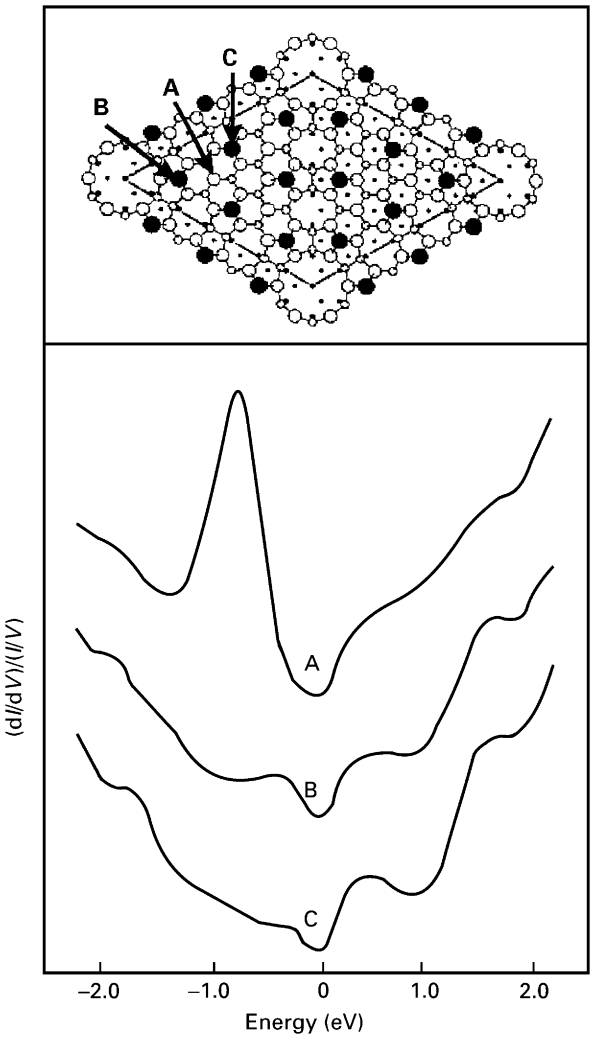

Figure 4 Atom-resolved spectra of the Si(111)-(7 × 7) surface obtained at positions indicated in the upper schematic. Reproduced with permission of the American Institute of Physics from Wolkow R and Avouris PH (1988) *Physical Review Letters* 60: 1049–1052.

Barrier Height Spectroscopy

Lack of direct knowledge of the effective height and width of the tunnelling barrier during spectroscopic measurements makes quantitative understanding of spectra difficult. Properties of the tunnelling barrier can however be investigated, giving information complementary to I–V spectroscopy. Barrier height spectroscopy consists of measuring the dependence of the tunnelling current on the tip–sample separation, at constant bias voltage. What is actually measured is the apparent barrier height, which is defined as

$$\Phi_{ap} = \left[\frac{1}{1.025} \cdot \frac{d(\ln G_t)}{dz}\right]^2$$

where G_t is the tunnelling conductance. Thus by measuring current as a function of tip–sample separation, G_t and Φ_{ap} can be calculated.

By applying a small modulation to the tip–sample separation (z) at constant bias voltage and constant tunnelling current, a lock-in amplifier can be used to measure dI/dz. The modulation frequency is chosen to be larger than the feedback loop bandwidth but smaller than resonant mechanical frequencies of the microscope. The dI/dz signal measured is directly related to the local surface work function and often provides useful contrast.

Another method of measuring the apparent barrier height is to record the tunnelling current directly as a function of tip–sample separation for a constant bias voltage. The tip–sample separation is reduced while the tunnelling current is measured. Although conceptually simple, there are experimental complications that must be taken into account. As the tip–sample separation becomes very small, the attractive forces between them tend to deform the tip and cause the actual separation to be smaller than expected. In fact, while point contact is typically used as the reference for tip–sample separation, this contact is usually realized with a jump to contact from a small separation. It can also be difficult to maintain a constant bias voltage, as the tip–sample separation becomes very small, since the junction impedance can become comparable to that of the current preamplifier causing a significant decrease in the actual bias voltage. By measuring the voltage across the junction as well as the tunnelling current this problem can be overcome. Figure 5 shows tunneling current and bias voltage as a function of tip–sample separation for a Au(110) sample and W tip (most probably covered with Au). The dramatic decrease in bias voltage at small tip–sample separations can be seen.

Inelastic Electron Tunnelling Spectroscopy

The majority of the tunnelling current consists of elastically tunnelling electrons. Inelastic pathways in which tunnelling electrons excite transitions can be used for recording local spectra. For a vibrational transition of a molecule contained in the junction this can occur above the threshold voltage of $|V| = \hbar\omega/e$ (Figure 6), where $\hbar\omega$ is the energy of a molecular vibrational transition, and e is the charge of an electron. Inelastic pathways effectively increase the available number of final states for a tunnelling electron, thus producing a kink in the I–V curve at $|V| = \hbar\omega/e$ for each vibrational transition excited. Using a similar modulation technique to that previously described d^2I/dV^2 vs. V can be measured directly with a lock-in amplifier (as the second harmonic

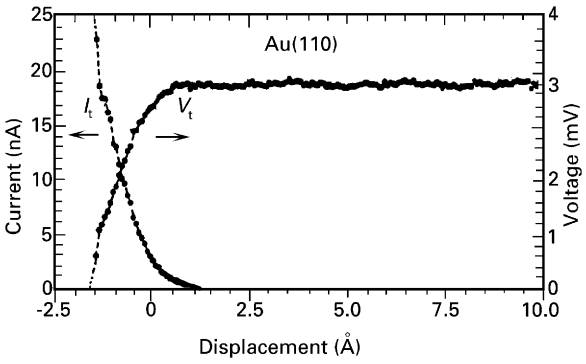

Figure 5 Tunnelling current (I_t), and bias voltage (V_t) during tip approach on Au(110). Reproduced with permission of the American Institute of Physics from Olesen L, et al. (1996) *Physics Review Letters* 76: 1485–1488.

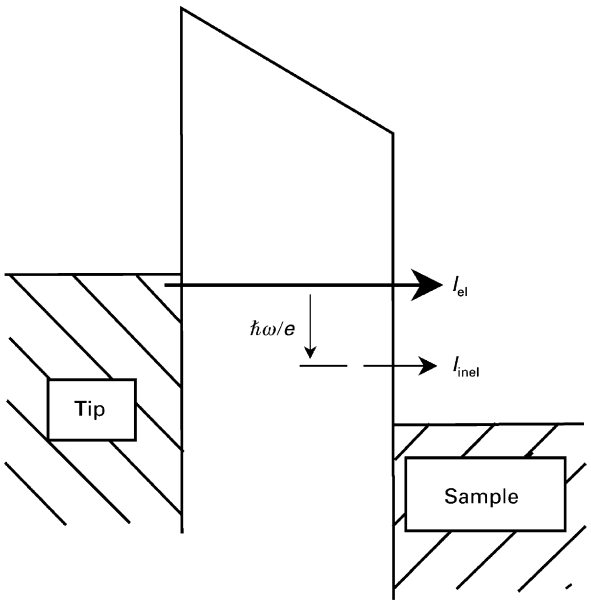

Figure 6 Energy level diagram for tip–sample tunnelling gap depicting both elastic (I_{el}) and inelastic (I_{inel}) tunnelling. Above the threshold voltage $|V| = \hbar\omega/e$ tunnelling electrons can excite a vibrational transition, for molecules in the tunnel junction. The densities of states of both tip and sample have been neglected for clarity.

of the modulation frequency). This has the benefit of transforming the kinks in I–V to peaks and dips in d^2I/dV^2 vs. V, some of which may be assigned to molecular vibrations (of energy eV). Vibrational spectra can be obtained in this fashion for molecules in metal–insulator–metal sandwich tunnel junctions at low temperature. Limiting peak widths of the observable features also requires low temperatures as in tunnel diodes and sandwich tunnel junctions. **Figure 7** shows inelastic electron tunnelling spectra of acetylene (C_2H_2) and perdeuterated acetylene (C_2D_2), adsorbed on Cu(100) at 8 K, and the difference spectrum. The spectrum of acetylene has a peak at 359 meV corresponding to the C = H stretch. This peak is shifted to 267 meV for the C = D stretch in perdeuterated acetylene. Tuning the bias voltage to the energy of the vibrational mode and monitoring d^2I/dV^2 allows vibrational spectroscopic imaging. **Figure 8** demonstrates vibrational spectroscopic imaging of acetylene and perdeuterated acetylene of Cu(100).

Inelastic electron tunnelling spectroscopy with the STM allows unambiguous chemical identification of surface species, as demonstrated above. Electronic spectroscopy is also capable of differentiating between limited sets of adsorbates but does not as a rule enable such determinations. The vibrational spectra of isolated molecules also shed light on the chemical environment and bonding changes of minority surface sites, and their critical role in surface processes, such as chemistry, corrosion, and film growth.

Photon Emission

Electrons tunnelling inelastically between tip and surface can induce photon emission from the tunnel junction. On some surfaces, the inelastic tunnelling is enhanced by exciting surface plasmons, which decay by emitting a photon. Measuring emitted photons as a function of applied bias voltage yields information analogous to conventional inverse photon emission experiments. Unlike conventional inverse photon emission experiments occupied and unoccupied electronic states can be probed with photon-emission STM by scanning positive or negative bias voltages, respectively. Dispersing the emission with a spectrometer allows the spectral fingerprint of a feature to be measured. The spatial resolution of the STM allows the emission spectrum of isolated molecules to be recorded.

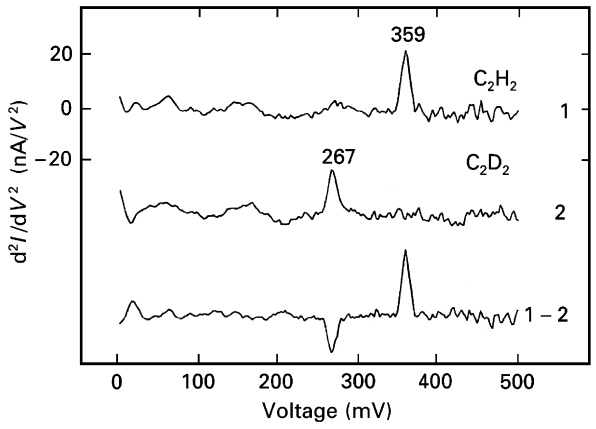

Figure 7 Inelastic electron tunnelling spectra of C_2H_2 (1) C_2D_2 (2) taken with the same STM tip and the difference spectra (1–2). Reproduced with the permission of the American Association for the Advancement of Science from Stipe BC, et al. (1998) *Science* 280: 1732–1735.

Instrumentation

Microscope

Design considerations for spectroscopy with the STM are the same as for the STM in general. Due to the exponential dependence of tunnelling current on tip–sample separation, vibration isolation is of critical importance. The most demanding of the techniques mentioned above, inelastic electron tunnelling spectroscopy, requires special vibration isolation down to the level of ~0.001 Å over a limited bandwidth and operation at extremely low temperatures (ca. 4 K). Various designs for vibration isolation have been implemented, from placing the STM on top of a Viton stack, to mounting the instrument on a pneumatically suspended laser table enclosed in an acoustic isolation chamber. The STM itself should be constructed rigidly so as to yield the highest possible resonance frequencies. Shielding from electronic noise is also important, but is determined primarily by the design of the control electronics as will be discussed below.

Other aspects of the microscope design depend upon the intended experiments. I–V spectra can be obtained in air, if the system to be studied is not air-sensitive. Investigation of isolated adsorbates on metal single crystals requires ultrahigh vacuum, to enable sample preparation, and often cryogenic temperatures, to limit thermally activated diffusion. Cryogenic cooling also reduces thermal drift allowing an area to be studied repeatedly.

Electronics

Low-noise electronics are important to maintain the stability of the probe tip and to avoid coupling of the control electronics to AC voltages powering the electronics or in nearby equipment. Proper shielding and planning can reduce the electronic noise to sufficiently low levels that this is rarely a limiting factor.

Blanking the feedback loop, which is required for many of the spectroscopic techniques discussed, is typically accomplished through the use of a sample-and-hold circuit. In normal operation, the STM maintains a

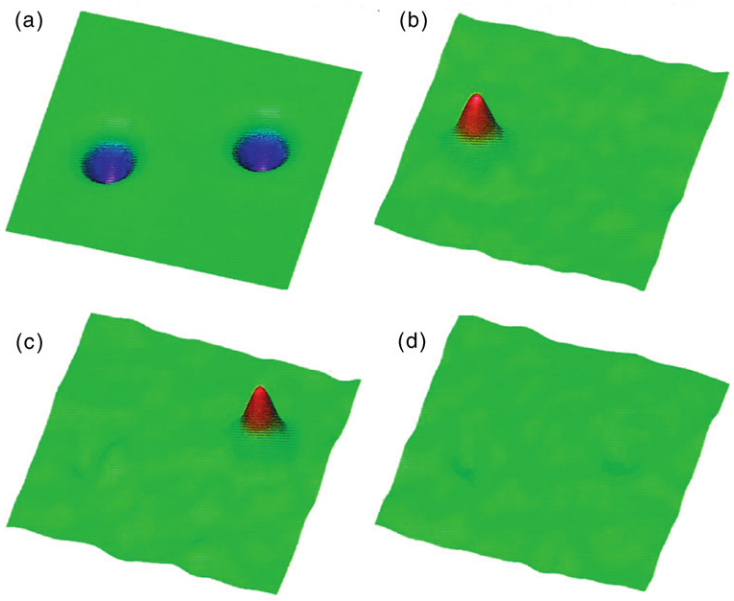

Figure 8 Vibrational spectroscopic imaging of C_2H_2 and C_2D_2. (a) Constant current STM image of a C_2H_2 molecule (left) and C_2D_2 molecule (right). The d^2I/dV^2 images of the same area recorded with a bias voltage of (b) 358 mV, (c) 266 mV, and (d) 311 mV, with a 10 mV modulation. All images are 48 Å × 48 Å with 1 nA DC tunnelling current. Reproduced with the permission of the American Association for the Advancement of Science from Stipe BC, et al. (1998) *Science* 280: 1732–1735.

constant tunnelling current by driving the z-piezoelectric transducer with the error signal generated from the difference of the tunnelling current (converted to a voltage by the preamplifier) and a reference voltage. A sample-and-hold circuit interrupts the input to the feedback control loop and thus maintains a constant voltage to the piezoelectric transducer controlling tip–sample separation. The applied z-piezoelectric voltage, can be held constant for up to several seconds with such a circuit. If longer blanking times are required, the use of a digital feedback blanking circuit can hold the voltage constant indefinitely. In addition, nearly constant drift can be corrected in microscopes where hold times are long compared to drift rates.

Microscope Probe Tip

Since the observed spectral features are a convolution of both the tip and the sample electronic density of states, understanding the role of the microscope probe tip in determining the observed spectra is critical to allowing interpretation of spectral features. A tip with a constant, preferably flat, density of states is typically desirable so that the sample's electronic structure dominates the spectral features observed. Alternatively a probe tip with a single sharp spectral feature can be useful in obtaining spectra.

Semiconductors have greatly varying densities of states and thus contributions from metal probe tips are less prominent. Metal surface state densities vary to a much smaller degree and are thus comparable to those of the tip states, making electronic spectroscopy of metals more complicated. To enable comparison between spectra obtained at various surface positions it is important that the tip structure, and thus density of states, remains constant between measurements. Rearrangement of the tip apex can greatly affect the observed spectra and thus lead to spurious data interpretation.

Heteroatoms adsorbed to the tip can also play a large role in determining the observed spectra. Many studies have shown that the transfer of an adatom or molecule to the STM tip can affect the observed topography, e.g. yielding atomic resolution on an electronically flat close-packed metal substrate. The spectroscopic effects can be even larger. Special care must be taken when probing semiconductor surfaces. Tip–sample contact resulting in some semiconductor material on the probe tip apex can give rise to odd effects, such as negative differential resistance (NDR). The tunnelling current between tip and sample normally increases with increasing bias voltage. If, however, there is a band gap on both the tip and sample, the tunnelling current can decrease with increasing bias voltage, due to the decrease in overlap of the density of states when the two band gaps are not aligned. Figure 9 is an I–V curve exhibiting NDR of MoS_2, with a tungsten tip that came in contact with the surface. By backing away from the surface and field cleaning the tip, I–V curves without NDR are again obtained.

Negative differential resistance can also be observed for surfaces with localized trap states. A tunnelling

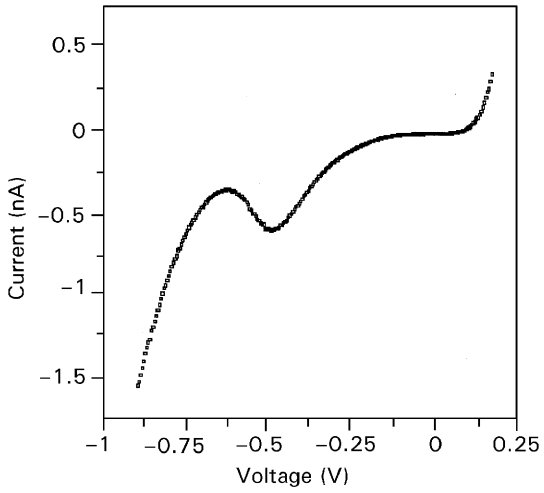

Figure 9 *I–V* scan of MoS_2 with a tungsten tip demonstrating negative differential resistance caused by the presence of MoS_2 on the tip. Kushmerick JG and Weiss PS, unpublished results.

electron can become localized for long times in these surface states, when they are in resonance with the Fermi level of the tip. Electrons so localized electrostatically repel other electrons causing a decrease in tunnelling current, referred to as a coulomb blockade. The voltage at which the NDR occurs is a measure of the energy of the localized trap state.

Other Scanning Probe Microscopes

Atomic Force Microscope (AFM)

It is possible to perform spectroscopy with SPMs other than the STM. The use of metal-coated cantilevers allows spectroscopic measurements with the AFM. The AFM maps surface topography by monitoring the attractive and/or repulsive probe–surface interactions as a surface is scanned by a cantilever. With a metal-coated cantilever, *I–V* curves can be obtained for surfaces incompatible for STM study, such as metal structures covered with an insulating oxide layer. The insulating film acts as a tunnelling barrier of constant width, allowing spectroscopic measurements analogous to constant-separation *I–V* scans.

Functionalization of a cantilever by deposition of a molecular film allows the chemical forces between molecules to be probed. The chemical force (bonding) between a functionalized cantilever and surface is measured by monitoring cantilever deflection while the sample approaches, makes contact with, then is drawn back from the probe. The deflection of the cantilever is then converted to a force from the cantilever spring constant. Figure 10 is a plot of force versus cantilever displacement curves for three combinations of tip and sample functionalization. The hysteresis in the curves is a measure of the adhesive interactions between probe and

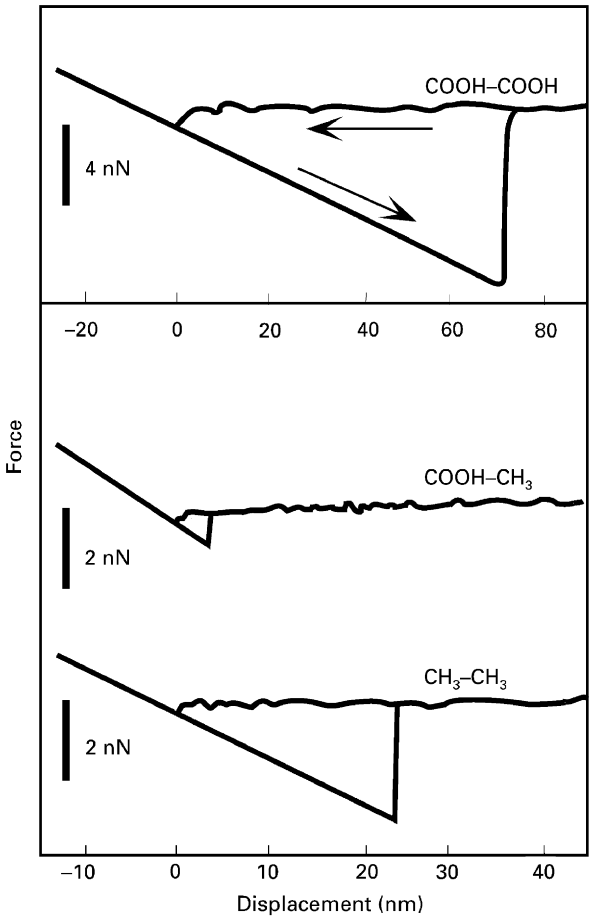

Figure 10 Force versus displacement curves recorded between functionalized atomic force microscope cantilever probes and surfaces. The adhesive interactions are strong for like–like interactions (COOH–COOH and CH_3–CH_3) but weak for interaction between unlike functional groups (COOH–CH_3). Noy A, Frisbie CD and Lieber CM, unpublished results.

sample. It can be seen that the strongest adhesion is when both the cantilever and sample are functionalized with the –COOH (hydrophilic) groups. Functionalization of the tip and sample with (hydrophobic) $–CH_3$ groups also yields a strong attractive interaction, but adhesion between –COOH and $–CH_3$ is minimal due to their smaller interactions. Such measurements are sometimes called chemical force microscopy.

Near-Field Scanning Optical Microscope (NSOM)

The NSOM also enables localized spectroscopic measurements. This technique circumvents the diffraction-limited resolution of conventional optical microscopy by scanning a light source or collector in close proximity to the surface of interest. A metal-clad optical fibre typically serves as the probe, allowing light to be either emitted or collected from its apex which is free of any metal

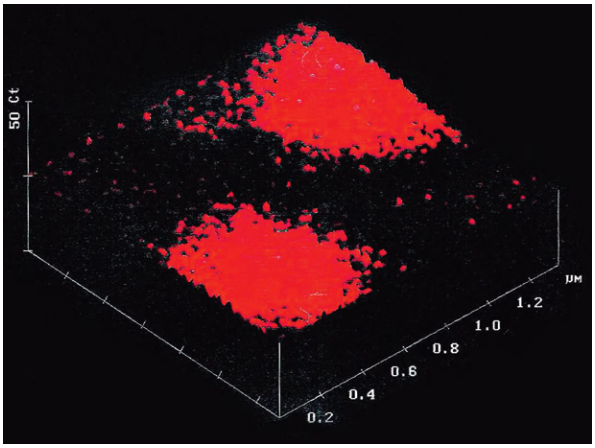

Figure 11 Fluorescence emission near-field scanning optical microscope image (1.3 μm × 1.3 μm) of a photosynthetic membrane fragment. Reproduced with permission of the American Chemical Society from Dunn RC, et al. (1994) *Journal of Physical Chemistry* 98: 3094–3098.

cladding. Other probes can also be used. By bringing the probe–sample separation into the near-field regime, the spatial resolution achieved is determined by the size of the unclad probe apex and can go well below the far-field limit of $\lambda/2$, where λ is the wavelength of light used. The NSOM can record absorption and fluorescence spectra, as well as measure the refractive index of surface and subsurface species. Spatial resolution of 12 nm has been achieved with visible light. While resolution is lower than that attainable with the STM, the ease of interpretation and familiarity of optical spectra make this technique attractive. Systems particularly suited to study with NSOM include unique biological structures such as the photosynthetic membrane shown in Figure 11.

If infrared absorption or Raman scattering is used as the contrast mechanism, vibrational spectra of samples can be obtained. The combination of the nanoscale spatial resolution of a scanned probe with the chemical specificity of vibrational spectroscopy allows *in situ* mapping of chemical functional groups with subwavelength spatial resolution. Figure 12 is a shear force image of a thin polystyrene film along with a representative near-field spectrum of the aromatic C–H stretch region recorded in the microscope with a 1 second integration time per point.

Also suitable for study are dopants in semiconductors and local structures in semiconductor lasers.

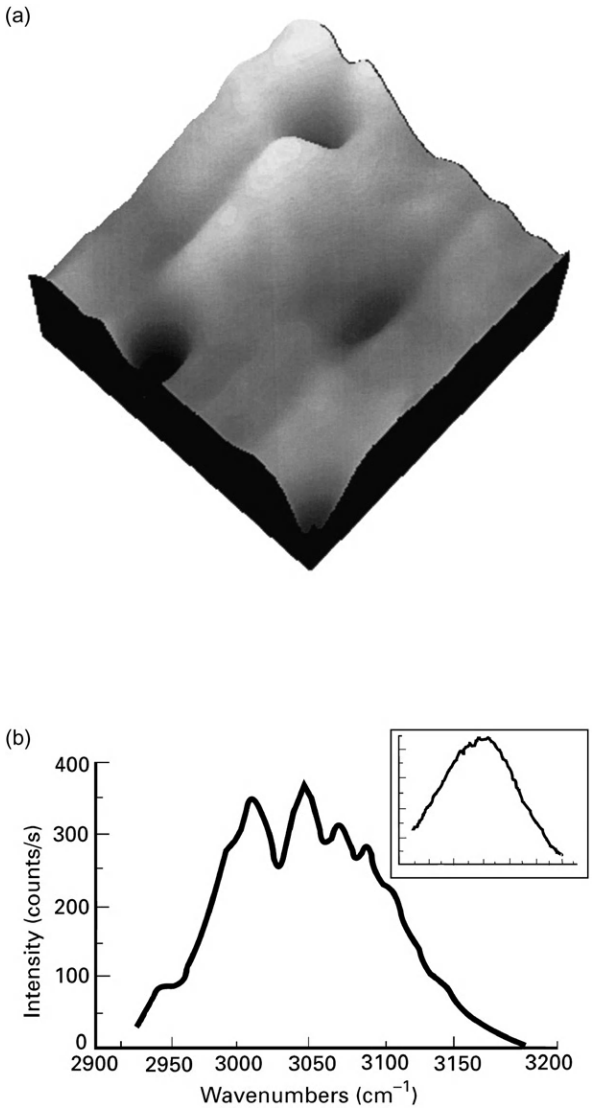

Figure 12 (a) A 3.1 × 3.1 μm shear force image of a thin polystyrene film deposited on a glass cover slip. The full-scale *z*-range is 62 nm. (b) Near-field IR transmission spectrum of a thin polystyrene film in the aromatic C–H stretching region. The inset is the laser output over the same spectral range in the absence of polystyrene absorption. Reproduced with permission of Stranick SJ, Richter LJ, Cavanagh RR, and Michaels C, unpublished results.

Overview

Spectroscopies with SPMs are being developed rapidly. The ability to study isolated or small structures of adsorbates has allowed incredible insight into the rich chemistry of surfaces, particularly the defining roles that defect-sites play. For example, in terms of imaging, technologies are now available for precise manipulation of material on surfaces and for positioning of specific atoms at specific locations, as published by Tseng and Li in 2007 (see Further Reading section). The demonstrations of single molecule vibrational spectroscopies with the STM and NSOM have further opened up new avenues for investigation.

See also: Inorganic Compounds and Minerals Studied Using X-Ray Diffraction, Inorganic Condensed Matter,

Applications of Luminescence Spectroscopy, Magnetic Force Microscopy, Scanning Probe Microscopy, Applications, Scanning Probe Microscopy, Theory, Surface Plasmon Resonance, Applications, Surface Plasmon Resonance, Instrumentation, Surface Plasmon Resonance, Theory, Surface Studies by IR Spectroscopy.

Further Reading

Betzig E and Trautman JK (1992) Near-field optics: Microscopy, spectroscopy, and surface modification beyond the diffraction limit. *Science* 257: 189–195.

Binnig G and Rohrer H (1986) Scanning tunneling microscopy. *IBM Journal of Research and Development* 30: 355–369.

Bonnell DA (ed.) (1993) *Scanning Tunneling Microscopy and Spectroscopy: Theory, Techniques, and Applications*. New York: VCH Publishers.

Chen CJ (1993) *Introduction to Scanning Tunneling Microscopy*. NewYork: Oxford University Press.

Feenstra RM (1994) Scanning tunneling spectroscopy. *Surface Science* 299/300: 965–979.

Sarid D (1991) *Scanning Force Microscopy: With Applications to Electric, Magnetic, and Atomic Forces*. Cambridge: Cambridge University Press.

Stroscio JA and Kaiser WA (1993) *Methods of Experimental Physics: Scanning Tunneling Microscopy*. New York: Academic Press.

Tseng AA and Li Z (2007) Manipulations of atoms and molecules by scanning probe microscopy. *Journal of Nanoscience and Nanotechnology* 7: 2582–2595.

Wiesendanger R (1994) *Scanning Probe Microscopy and Spectroscopy: Methods and Applications*. Cambridge: Cambridge University Press.